Non-intrusive performance monitoring method for air conditioners

Original Citation:
Non-intrusive performance monitoring method for air conditioners / Giannetti N., Yin J., Miyaoka Y., Talluri L., Milazzo A., Tanaka K., Kowa W., Saito K.. - In: INTERNATIONAL JOURNAL OF REFRIGERATION. - ISSN 0140-7007. - ELETTRONICO. - 181:(2026), pp. 74-83. [10.1016/j.ijrefrig.2025.10.003]

Published version:
DOI: 10.1016/j.ijrefrig.2025.10.003

Non-intrusive performance monitoring method for air conditioners

N. Giannetti[a], J. Yin[b], Y. Miyaoka[a], L. Talluri[c], A. Milazzo[c], K. Tanaka[d], W. Kowa[d], K. Saito[b]

[a] Sustainable Energy & Environmental Society Open Innovation Research Organization, Institute for Energy and Environmental system, Waseda University, Tokyo 169-8555, Japan

[b] Department of Applied Mechanics and Aerospace Engineering, Waseda University, Tokyo 169-8555, Japan,

[c] Department of Industrial Engineering, University of Florence, Florence 50139, Italy

[d] R&D Department, TEPCO Research Institute, Tokyo Electric Power Company Holdings, Inc., 4-1 Egasaki-cho, Tsurumi-ku Yokohama 230-8510, Japan

Abstract

A novel technique that relies solely on cost-effective and non-intrusive instrumentation for monitoring the performance of air conditioning installations in buildings was developed and experimentally tested. The proposed method addresses the challenges of field measurements in air-to-air units by using thermocouples and strain gauges placed strategically on the refrigerant pipeline of the outdoor unit to estimate the cycle COP. The tests demonstrated the feasibility of estimating refrigerant temperature and pressure without cutting the refrigerant pipeline. Real-time cycle COP deviations could be limited to 3% with proper calibration of the strain signal and the use of refrigerant properties. Additionally, compressor speed is identified through the frequency spectrum of the strain signal. Therefore, the refrigerant flow rate can be estimated using a compressor curve method that relies exclusively on simple instrumentation. Widespread adoption of this method could help close the knowledge gap between catalogue and field-operating performance of the numerous air conditioning installations.

Keywords: performance monitoring, air conditioning, building installation, non-intrusive instrumentation, strain gauge

1. Performance monitoring of air conditioners

The deployment of real-time performance monitoring techniques is pivotal to the digital transformation of air conditioning technologies. In particular, the ability to continuously assess system performance during field operation enables the development of optimized and adaptable dynamic control strategies, smart energy management systems (EMS), and predictive maintenance. These developments not only help reduce the cost and environmental impact of heating and cooling technologies—as integrated components of buildings—but also enhance their reliability and lifespan.

It is well recognized [1] that for field performance monitoring of air conditioners and heat pumps, the informative data available in literature (a) confirm largely dynamic operation, (b)quantify the occurrence of partial-load operation [2], and (c) highlight the discrepancy between efficiency values based on current testing standards and actual energy efficiency [3]. However, the actual real-time performance of air conditioners remains largely unclarified. Additionally, the practical application of digitalization technologies is limited due to the inadequate accessibility of real efficiency data, caused by improper testing methodologies and ineffective performance monitoring methods. Current rating standards rely on testing procedures which deactivate the native control of the tested unit and may be suitable to confidently define the hardware performance of the tested unit. On the contrary, operation performance within buildings may require broader characterizations to consider control features and performance interactions with building characteristics. Accordingly, while the software for EMS systems and digital twin technologies is being rapidly developed [4–8], the limited ability to verify the field performance of heat pumps and air conditioners may hinder the full realization of their potential to decarbonize heat utilization and supply.

Although electrical power consumption can be readily measured, heat is a form of energy transfer that carries diversified quality characteristics and is difficult to store, visualize, measure, and model due to its inherent multidimensionality and its tendency to interact with surrounding materials.

These challenges are often exacerbated in the case of air-to-air systems, for which the most common performance testing equipment relies on the measurement of the air-side thermal condition [2]. In this regard, emulator-type load-based tests [9–12] have been recently developed to address some of these challenges. Such testing methodology enables reproducible performance assessment of variable-speed air conditioners and heat pumps when operated under the same control as in field operation. The essence of this method is the integration of conventional testing equipment with numerical software that enables the mirroring of the thermal response of the conditioned space within a building with arbitrary features. This approach is pivotal for enhancing the representativeness of testing results, as detailed in references [13–15], and for the development of real-time performance monitoring systems. As the accuracy of thermal air-side measurements is affected by spatial variability in temperature and humidity conditions, bulky, intrusive, and costly equipment is required [16], making installation impractical for field operation monitoring [17].

Machine learning methods have demonstrated promising, accurate, and cost-effective characteristics for real-time performance monitoring. Sholahudin et al. [18–21] proposed and verified the use of thermocouples combined with a power meter for cooling capacity estimation and real-time performance monitoring of air-to-air systems. The scalability of these estimations across different systems was verified, achieving accuracy within approximately 10% of the recorded capacity [22]. However, machine learning methods rely on extensive training data collected during the testing phase, show limited generalizability, and may obscure the physical interpretation of results.

A recent report from the IEA's Annex 88 project on "Evaluation and Demonstration of Actual Energy Efficiency of Heat Pump Systems in Buildings" [23] categorizes monitoring methods for air conditioners as (A) indoor-side air enthalpy difference methods, (B) outdoor-side air enthalpy methods, and (C) refrigerant-specific enthalpy difference methods. In addition, T/CAS 305-208 [24] and ASHRAE Standard 221-2020 [25] are available. Within category (A), the indoor-side air enthalpy difference method mainly includes the "indoor unit external air hood method" [26] and the "indoor unit outlet air sampling method" [27]. The outdoor-side air enthalpy method (B) addresses the potential interference from users with data collected using indoor-side methods, and includes the "static multi-port air sampling method" [27–28], the air hood method [29], which has shown relative errors of up to 15%, and both static [30–31] and dynamic [32] "outlet air sampling methods."

Finally, refrigerant-specific enthalpy difference methods (C) include the "refrigerant mass flow meter method" [33–34], the "throttling model method" [35], the "compressor energy conservation (CEC) method" [36–39], the "compressor performance curve method" [40], and the "compressor volumetric efficiency (CVE) method" [41], which has shown total errors over 20%, increased error during transient operating conditions, and relatively smaller error during steady operation. However, the accuracy of this method depends on the precision of the volumetric efficiency of the compressor, which in turn relies on fundamental data supplied by the manufacturer. Additionally, results may be affected by compressor wear and deterioration during long-term operation [23]. Accordingly, the unresolved challenges in existing performance monitoring methods include (i) interference of sensors with occupants' indoor activity, (ii) bulkiness, (iii) high sensor costs, (iv) disruption of system operation during sensor installation, and (v) limited accuracy due to airside spatial uncertainties or problematic refrigerant-side flow rate measurement under two-phase and dynamic conditions.

In principle, the efficiency of a thermodynamic cycle can be calculated from the knowledge of few thermodynamic states of the refrigerant. This often translates in the need for reliable estimations of refrigerant temperature and pressure. Temperature is often approximated to the value measured on the outer surface of the refrigerant pipeline and saturation pressure may be derived from temperature measurements in phase transition areas, but such an approach often requires neglecting pressure drop. Reliable pressure measurements are critical for various applications, spanning across environmental monitoring [42-43], industrial processes [44], and engineering systems [45-46] to ensure safe and efficient operation. Common methods to measure pressure include manometers (e.g. [47-48]) and mechanical pressure gauges. In the latter case, elastic elements that deform with the application of pressure are used. The deformation can alter the capacitance of a diaphragm [49], activate a piezoelectric sensor [50], or produce a measurable strain [51-52]. Unfortunately, pressure measurements require invasive techniques to install additional sensors, and generally, their applicability to in-situ performance monitoring of heating and cooling technologies is limited [53]. In fact, unless the system already has pressure instrumentation, the placement of pressure plugs would require interrupting operation and cutting the refrigerant pipeline. Tran et al. (2013) [54] proposed an alternative method but still required a pressure sensor installed at the refrigerant charging plug.

Whenever the performance representation provided by the thermodynamic cycle is insufficiently accurate and the energy expenses deriving from auxiliaries are not negligible, the system performance assessment requires estimations of the capacity supplied by the system. Cooling or heating capacity can be calculated from the enthalpy difference of the refrigerant through the indoor heat exchanger, that is the specific enthalpy difference multiplied by the refrigerant mass flow rate. Mass flow rate measurements can be reduced to compressor frequency measurements once the compressor inlet state, vane volume, and volumetric efficiency are known. Generally, frequency measurements rely on Hall effect sensors [55] and other non-contact optical methods [56]. Recently, innovative acoustic methods have been proposed in literature [57].

This study addressed the main unresolved challenges in performance monitoring, by developing and validating a non-intrusive method for monitoring the performance of air conditioners, providing accurate performance estimations with negligible instrumentation costs. Specifically, a physical representation of the refrigerant cycle was obtained by using thermocouples and strain gauges strategically placed on the external surface of the refrigerant pipeline in the outdoor unit to estimate refrigerant temperature and pressure [58], without interfering with system operation. Finally, an alternative method for estimating the refrigerant flow rate from the Fast Fourier Transform (FFT) of the strain signal and compressor volumetric efficiency is proposed for determining the system COP. In this manner, in-situ performance monitoring can be realized while minimizing the required instrumentation cost and excluding invasive instrumentation.

2. Cycle monitoring from thermocouples and strain gauges

Vapor compression systems share common fundamental working principles based on the cyclic circulation of a working fluid for continuous operation (Fig. 1). Because airside thermal measurements may be inaccurate unless bulky, intrusive, and expensive instrumentation is used, the method proposed in this study is based on identifying the refrigerant cycle and refrigerant mass flow rate using thermocouples and strain gauges strategically placed on the refrigerant pipeline of the outdoor unit, thereby avoiding interference with system operation and user activity. The surface temperature of the refrigerant pipeline from the thermocouples may represent the modulation of the refrigerant temperature along the cycle. Furthermore, correspondingly placed strain gauges may capture pressure modulations from the strain signal in the time domain after compensation for thermal expansion due to temperature variations (Fig. 1). In addition, if thermocouples are placed in areas where a two-phase refrigerant is expected to flow, they may estimate the refrigerant saturation pressure.

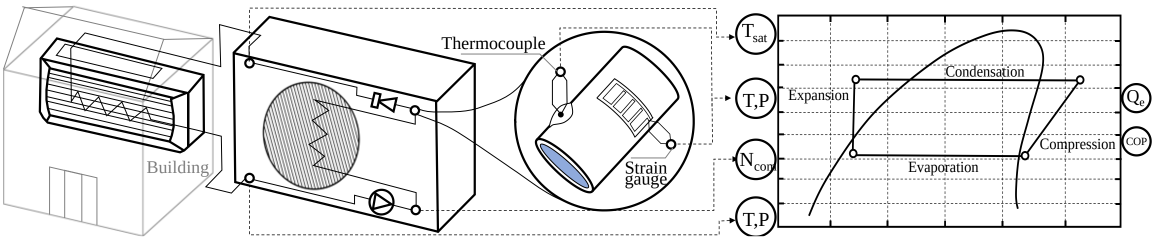

Fig.1 Conceptual illustration of the proposed performance measurement methodology.

In the following, the possibility of performing real-time cycle COP monitoring is demonstrated by calibrating the strain signal and temperature measurements to estimate refrigerant pressure and enthalpy. Finally, the frequency spectrum of the tube strain signal can be used to capture modulations in compressor speed, and combined with the compressor curve method to estimate system COP.

3. Experimental setup

The emulator-type testing methodology [9] was used to obtain reproducible reference data that included dynamic modulations of temperature, pressure, and cooling capacity, based on the native control of the tested unit operating within a virtual building defined by thermal inertia and subjected to a thermal load, as summarized in Table 1. As schematically shown in Fig. 2, the testing facility included two psychrometric rooms, where the indoor and outdoor units of the air conditioner were installed as they would be in an actual building. Figure 3 includes photographs of the actual setup of the tested outdoor and indoor units. The real-time cooling capacity supplied by the indoor unit was measured using the air-enthalpy method, while the outdoor unit was equipped with sufficient sensors (including temperature and pressure) to reconstruct the refrigerant-side performance of the system and verify the estimations derived from the thermocouples and strain gauges placed at predefined locations on the refrigerant pipelines of the outdoor unit. The refrigerant cycle provides essential information on the system's efficiency.

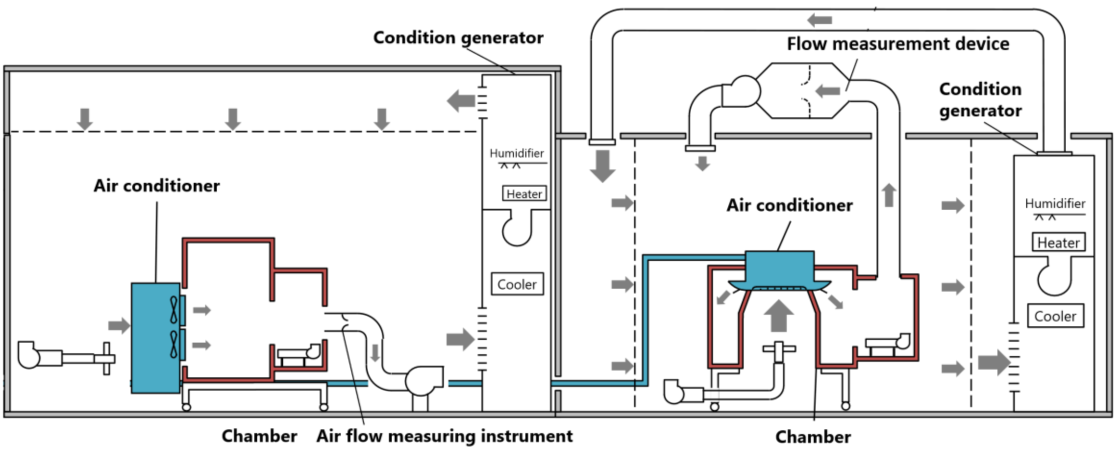

Fig. 2 Schematic diagram of the air-enthalpy setup in the outdoor (left) and indoor (right) psychrometric rooms.

Fig. 3 Photographs of the tested system in the outdoor (left) and indoor (right) psychrometric rooms with the corresponding measuring chambers.

In this study, the physical relationship between the total strain, thermal strain, and temperature of the pipeline, along with the refrigerant pressure, was used to develop a pressure sensor and subsequently estimate the refrigerant enthalpy based on its thermophysical properties. The specific enthalpy and pressure values extracted at strategic locations along the refrigerant cycle can be directly used to estimate the cycle COP (Eq. 1), where h_{EO}, h_{EI}, h_{CO}, and h_{CI} are the outlet and inlet enthalpies of the evaporator and condenser, respectively.

$$COP_{cycle} = \frac{Q_{Cooling}}{W} = \frac{h_{EO} - h_{EI}}{h_{CI} - h_{EO}} \quad (1)$$

The instrumentation setup (including the thermocouples, strain gauges, and pressure sensors) is schematically shown in Fig. 4. The sensor specifications are summarized in Table 1. The strain gauges and thermocouples were installed on the surface of the refrigerant pipelines at the inlet and outlet of the compressor and the expansion valve, which correspond to the four corners of the refrigerant cycle. Although it may be argued that, in principle, refrigerant pressure can be estimated from the saturation temperature, the reversed operation of the system in heating mode would require an additional thermocouple to be placed in the two-phase area of the indoor heat exchanger. The installation of this additional sensor may momentarily interfere with the indoor activity of the occupants. Additionally, the proposed approach allows for the estimation of pressure drop across both high- and low pressure sides of the cycle, whereas the pointwise estimation of the saturation pressure through temperature measurement would disregard pressure drops.

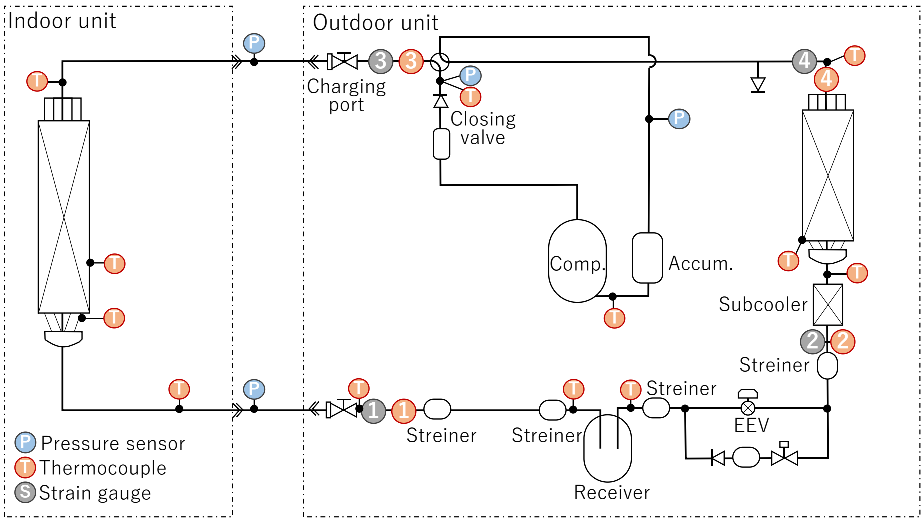

Fig. 4 Schematic diagram of the complete set of instrumentation, indicating the position of sensors on the refrigerant pipelines.

Table 1 Sensor specifications, range, and accuracy

Sensor type	Model	Range	Accuracy
Pressure sensor	YOKOGAWA/FP201	0 – 5 MPaG	±0.25% of full range
Thermocouple	Ninomiya/0.32 x1P T-2-G-J2 (T-G)	-40 – 90 °C	±0.5 K
Strain gauge	RS PRO Wire Lead Strain Gauge 5mm 120Ω	-30 – 80 °C	G 2.1±1% (-), φ ±1%, A ±0.1%

Sets of thermocouples and strain gauges were installed in close proximity to locally estimate the thermal strain of the pipeline while minimizing inaccuracies due to heat losses and longitudinal conductive heat transfer. The bends of the pipeline were avoided to ensure accurate circumferential strain measurements (Fig. 5, left). As shown in Fig. 5, to minimize signal interference, the strain gauge wires were twisted to reduce crosstalk and maintain signal symmetry. Additionally, aluminum foil was wrapped around the wires and the strain signal collector to shield them from electromagnetic interference caused by external electromagnetic sources. Furthermore, to address the sensitivity of the strain gauges to environmental humidity, the installation points were insulated to protect against humidity changes and the formation of condensation.

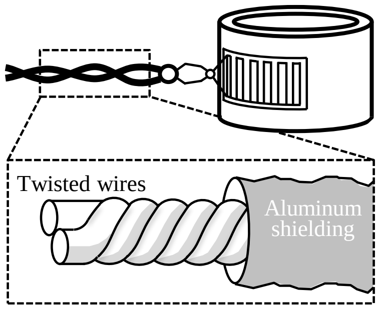

Fig. 5 Schematic of strain gauge installation on the outer surface of the refrigerant pipeline with twisted wires and aluminum shielding for external signals and humidity.

The setpoint indoor temperature was 25 °C, and the thermal load introduced by occupants and heat infiltration from the external environment accounted for 30% of the system's nominal cooling capacity. The tested unit was a ceiling-type system with a design cooling capacity of 10 kW, using R32 refrigerant (Table 2), virtually installed in a 147 m^3 indoor space, simulated in its thermal response by the room emulator. In fact, the thermal response of the indoor temperature and humidity in a conditioned environment is also related to the heat and moisture capacities of the air, fixtures, and walls of the room. Namely, during dynamic operation, unlike steady-state operation, the "building load" and the "air conditioning capacity" are not necessarily equivalent. For a given unbalance between load and supplied capacity, the room air temperature experiences variations at a rate that is defined by the heat capacity of the room. Therefore, the assessment of the dynamic performance of the air conditioner signifies clarifying its control characteristics and their interaction with the building thermal features. Hence, the dynamic performance of air conditioners cannot be reproducibly tested unless the "room-side air condition" is reproducible across different laboratory settings.

In the present study the volume of the proposed testing methodology, the heat capacity of the entire virtual room was set to be approximately 10 times that of the indoor air. This choice is guided by the empirical estimations and technical practices reported in [27,28].

Data were collected under the operating conditions listed in Table 3. Specifically, the air conditioner was operated in cooling mode with a constant outdoor temperature and relative humidity of 35 °C and 40%, respectively.

Table 2 Tested unit

Indoor unit type	Refrigerant	Design cooling capacity	Design heating capacity
4-port ceiling type	R32	10.0 kW	11.2 kW

Table 3 Test conditions for preliminary investigation of gauge pressure estimation

Room heat capacity	Load	Outdoor temperature	Outdoor relative humidity	Indoor set temperature
2410 kJ/K	30 %	35 °C	40 %	25 °C

While operating under such low-load conditions, the native control was unable to stabilize the system's operation and to stably converge the room temperature to the set point. As a result, the compressor operated with on-off cycles, represented by the cooling capacity modulations shown as grey empty markers in Fig. 6, which caused cyclical variations of the indoor temperature within an interval around the setpoint.

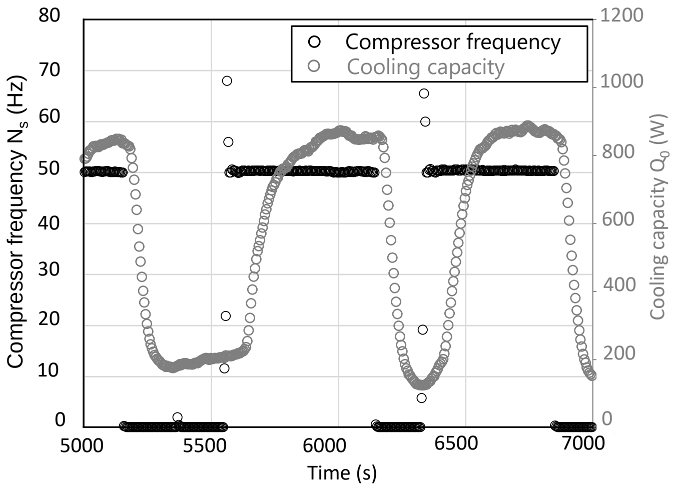

Fig. 6 Example of recorded on-off cycling modulations of the Compressor frequency (black markers) and cooling capacity (grey markers) from the collected data at 30% partial load ratio in the test conditions of Table 3.

4. Data reduction and gauge pressure estimation

Although the thermocouples placed on the refrigerant pipeline of the outdoor unit provided a direct estimation of the local refrigerant temperatures, the strain signal (Eq. 2) from the corresponding strain gauges does not immediately reflect refrigerant pressure modulations.

$$e = \frac{dr}{r} \tag{2}$$

Equation (2) represents the total radial strain, which is the relative variation in radius r due to the tension arising from changes in the local refrigerant state. Part of this radius variation is associated with the thermal expansion of the pipeline (Eq. 3), while the remaining strain is related to the force generated by refrigerant pressure modulations and is calculated using Eq. (4). In the following calculations, the thermal expansion coefficient (β) of copper is taken as 0.000017 K^{-1}.

$$e_T = \frac{dr_T}{r} = \beta \Delta T \tag{3}$$

$$e_p = e - e_T = e - \beta \Delta T \tag{4}$$

Figure 7 shows that, by correcting the total strain signal (black empty markers) with the thermal strain e_T (red markers), as indicated by Eq. (4), the corrected strain e_p (grey markers) closely aligns with the pressure signal obtained from the pressure sensor placed at the compressor inlet (gray empty markers). Accordingly, the corrected strain signal e_p may be converted to estimate the gauge P_g and absolute pressure P modulations, as shown in Eq. (5), where t is the pipeline thickness and E is the Young's modulus of copper.

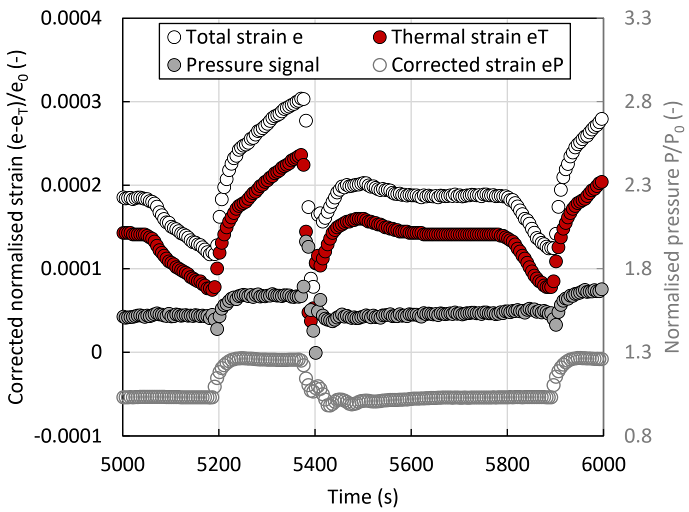

Fig. 7 Total-, thermal-, and pressure- strain signals (left axis) at the compressor inlet position, and directly measured pressure modulations (right axis) at the test conditions specified in Table 3.

The proposed formulation relies on the thin-wall approximation [59], which assumes one-dimensional radial expansion, although for a pressurized pipe the deformation is inherently biaxial. The approximation is reasonably accurate for diameter-to-thickness values higher than 10 [60] and the placement of the strain gauges should be planned accordingly. For the selected pipeline locations of the strain gauges in the present case, the diameter-to-thickness ratio was between 10-20.

$$P = P_0 + P_g = P_0 + \frac{(e - \Delta T * \beta)Et}{r} \quad (5)$$

The converted gauge pressure P_g is plotted in Fig. 8 and compared with the refrigerant pressure measured at the compressor inlet position (gray empty markers).

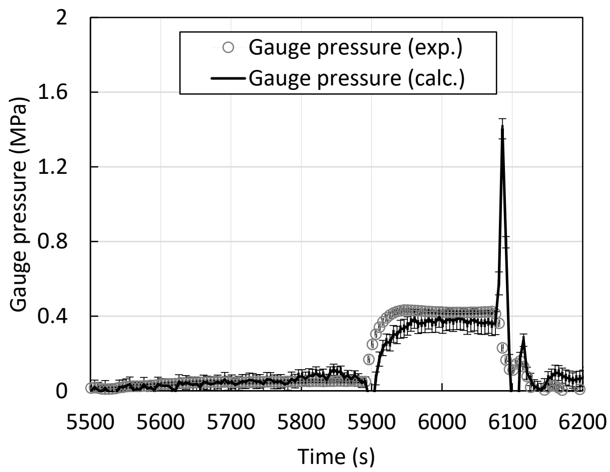

Fig. 8 Estimation of the gauge pressure P_g in an on-off cycling period from the derived pressure strain signal as compared with the value measured at the compressor inlet position, for the test conditions specified in Table 3.

To estimate the uncertainty of pressure estimations u_P, first the root sum of squares method was used to combine independent uncertainties of the measured strain u_e. Specifically, the uncertainty of the gauge factor (G 2.1±1%, from the catalogue specifications of the strain gauge [61]) was coupled with an additional 1% related to the possible misalignment φ occurring during installation, and a contribution arising from the amplifier (A 0.1% [62]). As a result, the strain uncertainty u_e was approximately 1.42%. Consequently, the uncertainty of the pressure estimates u_P (Eq. 5) was calculated according to error propagation from the measured strain e, the assumed variability of the Young's modulus E and thermal expansion coefficient β of copper [62], and the temperature variation ΔT, as expressed in Eq. (6).

$$u_P = \sqrt{\left(\frac{Et}{r}\right)^2 u_e^2 + \left(\frac{-\beta Et}{r}\right)^2 u_{\Delta T}^2 + \left(\frac{-\Delta TEt}{r}\right)^2 u_\beta^2 + \left[\frac{(e-\Delta T*\beta)t}{r}\right]^2 u_E^2 + u_{P0}^2} \quad (6)$$

Consistency between the calculated and experimental values was observed, with an average relative error of approximately 3.5% over the explored range with an average uncertainty of ±7.4 kPa. Larger errors may occur locally when the rapid dynamics of compressor operation are accompanied by slower thermal and mechanical stress responses. Consequently, a simple signal calibration can yield more accurate pressure estimations. The reference pressure P_o, connected to the rest installation state of the strain gauge, is required to estimate the absolute pressure P (Eq. 5). Alternatively, as the value of P_g is unaffected and may be offset by any known value of the local absolute pressure, a fair reference value may be extracted by considering the saturation pressure obtained from the thermocouples placed in the areas of the heat exchanger where a two-phase flow of the refrigerant is expected during cooling operation. Nonetheless, the challenges arising from obtaining effective and simple estimations of this parameter may require further investigation.

5. Performance estimation

Assuming an isenthalpic expansion in the expansion valve, and that two-phase refrigerant temperature measurements from opportunely placed thermocouples indicate the corresponding saturation pressure, the thermocouples and strain gauges placed on the pipeline of the outdoor unit may provide sufficient information to reconstruct the refrigerant cycle (Fig. 9). Such representation is sufficient for extracting the cycle coefficient of performance COP_{cycle} of the air conditioner, as defined in Eq. (1).

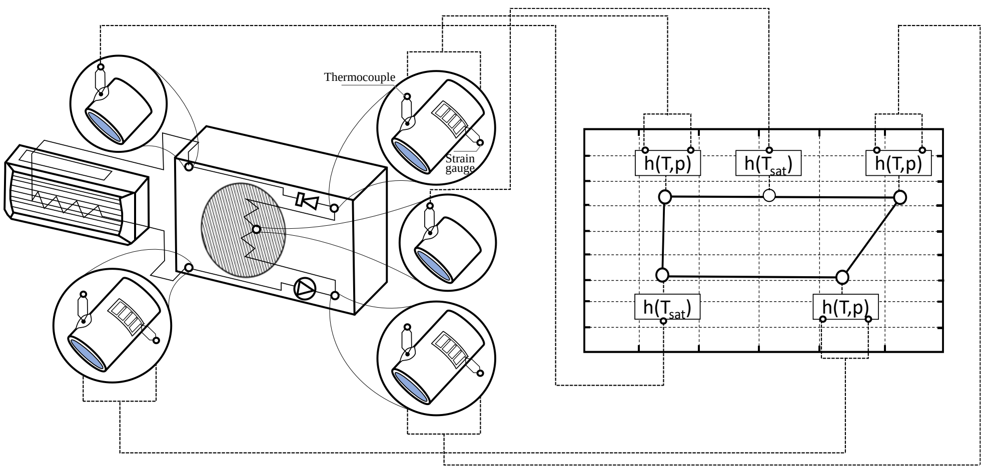

Fig. 9 Conceptual representation of the sensors required for refrigerant cycle identification from thermocouples and strain gauges placed on the refrigerant pipeline of the outdoor unit.

This method may be simplified by neglecting the pressure drop in the heat exchanger or by placing additional thermocouples in areas of the heat exchanger where two-phase flow is expected, relying on saturation pressure estimations from refrigerant properties. However, the placement of thermocouples on indoor heat exchangers should be limited in operational field installations to avoid disturbing the occupants' indoor activity during installation in operating units. In such cases, an optimal compromise may involve using strain gauges at required locations to obtain sufficient pressure estimations for capturing the cycle COP during reverse heating operation.

The magnitude of the strain was calibrated by introducing corrective coefficients for the temperature and strain offsets, and by modifying the relationship between the strain, refrigerant temperature, and refrigerant pressure, as expressed in Eq. (7).

$$P = P_0 + P_g = P_{ini} + \frac{((e+a)c-(\Delta T+b)\beta d)Et}{r} \quad (7)$$

Here, a and b are the calibration factors for the offset of the measured strain and refrigerant temperature, respectively, whereas c and d adjust the magnitudes of the measured and thermal strain values. Values of a and b (in K) close to 0, and c and d values close to 1, indicate negligible correction. Figure 10 illustrates the effect of this recalibration on strain measurements taken near the compressor inlet. Table 4 summarizes the corresponding corrective coefficients. Accordingly, the average relative error was limited to 1.4% in the explored range.

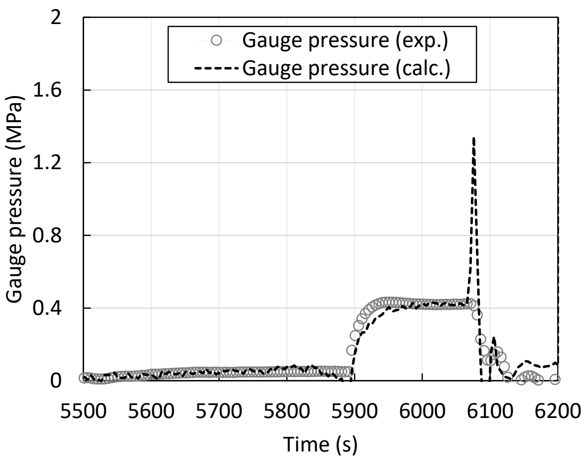

Fig. 10 Recalibration of the estimated gauge pressure P_g in an on-off cycling period as compared with the refrigerant pressure measured at the compressor inlet position, at the test conditions specified in Table 3.

Table 4 Recalibration coefficients for pressure estimation from strain and temperature measurements at the compressor inlet.

a	b	c	d
$-2.52 \cdot 10^{-7}$	0.367 (K)	0.961	0.905

Correspondingly, the refrigerant enthalpy was estimated under single-phase conditions by referring to the temperature and pressure values derived from the thermocouples and strain gauges placed on the external surface of the refrigerant pipeline, using the thermophysical properties of the R32 refrigerant. Figure 11 illustrates the precision of this enthalpy estimation at the compressor outlet by comparing the estimated value with that obtained from direct temperature and pressure measurements. Enthalpy estimation at the corners of the refrigerant cycle using REFPROP10 [64] and the assumption of isenthalpic expansion through the expansion valve enables cycle COP assessment and verification with direct experimental measurements under the testing conditions defined in Table 5.

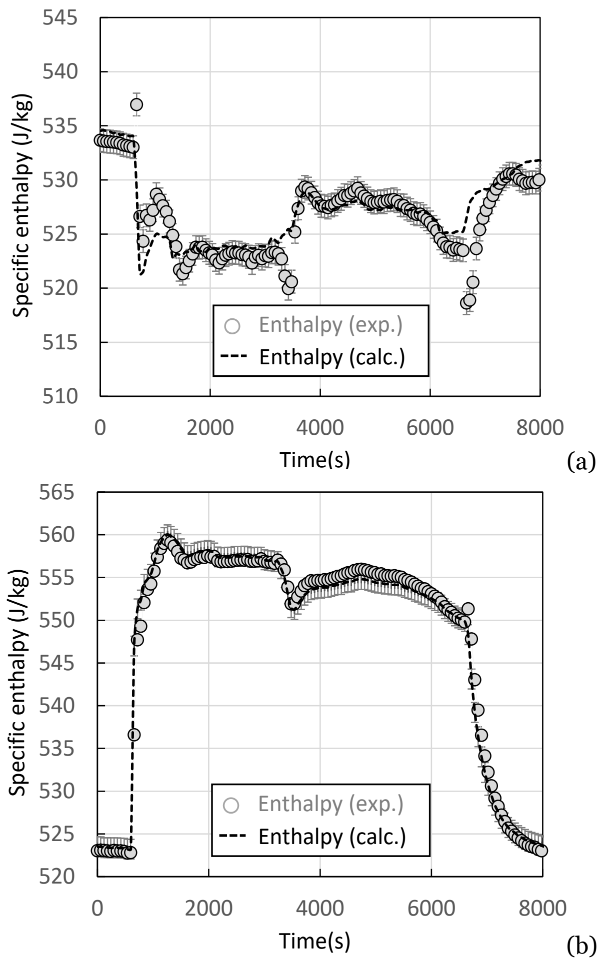

Fig. 11 Enthalpy estimation at the compressor inlet (a) and outlet (b) from temperature and pressure from thermocouples and strain gauges (dashed line) as compared with the enthalpy extracted from direct

measurement of refrigerant pressure and temperature at 35% partial load ratio in the test conditions reported in Table 4.

Table 5 Test conditions for performance estimation.

Building inertia	Load	Outdoor Temperature	Indoor set temperature	Sensible Heat Factor
2410 kJ/kg	37.5%	29 ºC	27 ºC	0.85

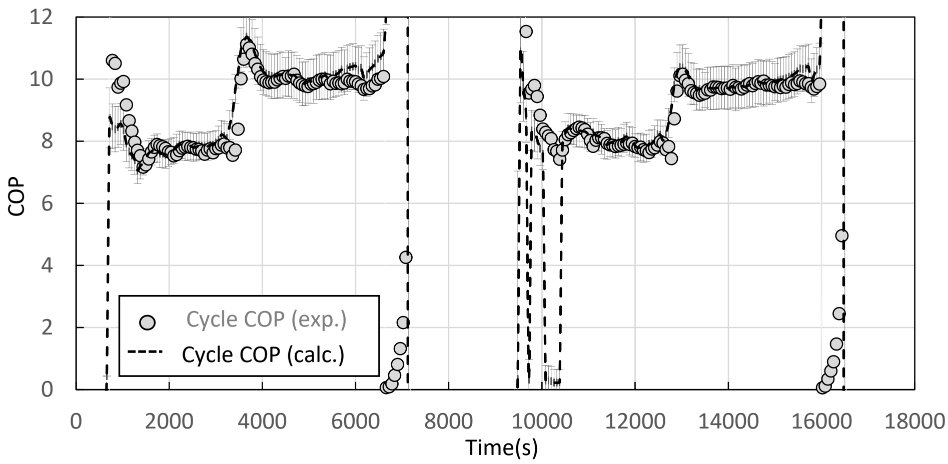

Fig. 12 Estimation of the cycle COP at 35% partial load ratio as compared with the direct measurements from the testing facility for the testing condition defined in Table 4. Error bars refer to the calculated COP (dashed line).

Under these conditions, the system operates in on-off cycling mode, and Fig. 12 shows the real-time cycle COP estimated and measured during such cycling operation. The relative estimation error during the active part of the first cycle in Fig. 12 remained below 2.9%, with an average uncertainty within $\pm 6.9\%$, demonstrating the high accuracy achieved using simple, non-intrusive, and inexpensive instrumentation.

Compressor speed from the frequency spectrum of the pipeline strain signal

The use of strain gauges also enables the capture of dynamic operational characteristics of the system. Specifically, the Fast Fourier Transform technique (FFT) can be applied to the time-domain strain signal of the pipeline to extract its frequency spectrum and monitor the compressor speed. Measuring this fundamental control parameter is critical for estimating the system's output cooling and heating capacities, which can be derived using either machine learning methods or a compressor curve method—provided the compressor's volumetric efficiency is known and combined with the refrigerant states identified by the

non-intrusive instrumentation described above.
To identify the noise signals superimposed on the strain signal, measurements were first performed with the system in an inactive state. When the measurement was repeated with the compressor stably operating at 76.7 Hz, the FFT of the strain signal for both inactive and active system conditions was obtained, as shown in Fig. 13. The active system signal (black line) was first compared with the noise from the inactive system signal (gray line) to exclude lower-order amplitudes from the frequency spectrum. Subsequently, the additional peaks appearing in the spectrum of the active system signal were compared with the experimental measurements of the compressor speed. This confirmed that the compressor speed could be identified from the frequency spectrum of the strain signal.

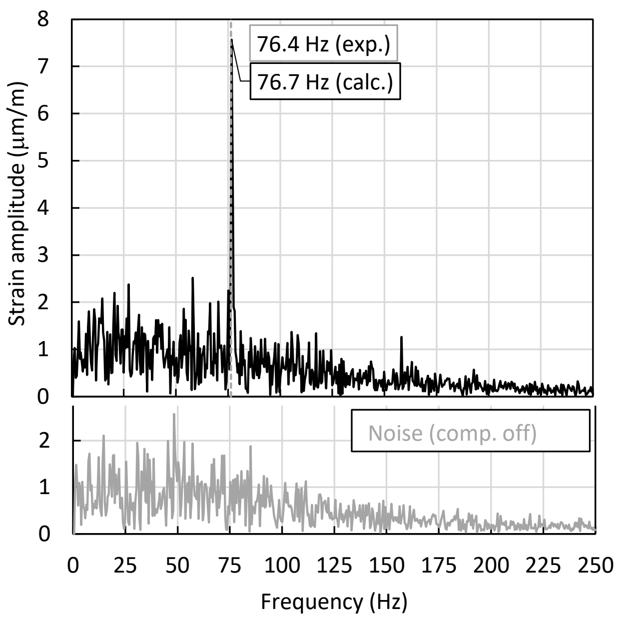

Fig. 13 Frequency spectrum of the measured strain signal when operating the compressor at 76.4 Hz.

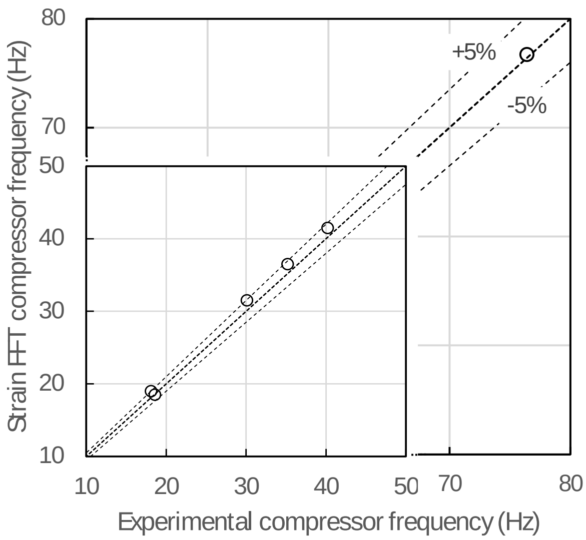

Fig. 14 Estimation of the compressor speed from the frequency spectrum of the measured strain signal in various compressor operating conditions.

Figure 13 shows the frequency spectrum of the background noise signal obtained from the discrete-time strain signal at the compressor outlet. The sampling interval (0.002 s) was selected according to the Nyquist–Shannon sampling theorem [65] to properly capture the frequency range of interest ($f < 250$ Hz) with a 1Hz frequency resolution, while limiting the amount of data requires. The direct experimental measurement indicated a compressor speed of 76.4 Hz, and the frequency spectrum of the strain signal at the compressor outlet showed a corresponding peak with an amplitude of 7.5 μm/m at 76.7 Hz (with smaller amplitude peaks at multiple frequencies). It was also demonstrated that similar accuracy can be achieved in a reasonably wide range of conditions for technical implementation (18.1 – 76.4 Hz) and with sufficient repeatability at corresponding conditions (see Fig 14). However, the accuracy of such compressor speed measurement method during transient operation is still to be quantified and the influence of other sources of error (such as the strain gauge position, structural properties of the pipeline, or noise from other components) should be further investigated.

6. Conclusions

A novel technique that relies solely on cost-effective and non-intrusive instrumentation for monitoring the performance of air conditioners was developed and experimentally tested. The proposed method addresses the challenges of field measurements for air-to-air units by using thermocouples and strain gauges strategically placed on the refrigerant pipeline of the outdoor unit to estimate the temperature and pressure required for identifying the working

cycle COP. Interference of sensors with occupants' indoor activity was avoided with low-cost and small sensors that can be installed without disruption of system operation. As a result, the proposed methodology enabled in-situ performance monitoring with minimal instrumentation cost and, by decoupling pressure estimation from saturation temperature measurements, could also be applied to reversible units during heating operation.
Preliminary tests demonstrated the practicability of refrigerant temperature and pressure estimations without the need for cutting the refrigerant pipeline.
Correspondingly, real-time cycle COP can be assessed from the enthalpy values derived using the thermophysical properties of the refrigerant. As a result, cycle COP deviations can be limited to within 3% of the experimental value through calibration of the strain signal and application of refrigerant properties. The method also offers a scalable physical representation applicable to various systems—not limited to air-to-air units. This suggests the potential for effective real-time performance monitoring of vapor compression system installations. However, this performance index assumes negligible electrical consumption of auxiliary components, which may only partially represent the system performance, especially under low-load operation.
Accordingly, compressor speed was identified through the frequency spectrum of the strain signal. Such approach may be used to estimate the refrigerant flow rate via a compressor curve method based solely on this simple instrumentation and obtain the system COP from the measurement of the total power consumption of the system. Alternatively, it may be integrated with machine learning techniques to reconstruct complex physical relationships between system performance and measured parameters.
Widespread adoption of this method could help close the knowledge gap regarding the real-world operational performance of the numerous air conditioners installed globally in buildings.

References

[1] Matsui, E., Kametani, S., Nobe, T., 2016. Accuracy Improvement of Performance Evaluation for Variable Refrigerant Flow Systems. Proceedings of ECOS, 424-432.
[2] Building Research Institute, 2011. Report of Committee for Actual Energy Performance of Room Air Conditioners. 28th February 2011 (in Japanese).
[3] Won, A., Ichikawa, T., Yoshida, S., Sadohara, S., 2009. Study on running performance of a split-type air conditioning system installed in the national university campus in Japan. J. Asian Archit. Build. Eng. 8, 579–583.
[4] Drgoňa, J., Arroyo, J., Cupeiro Figueroa, I., Blum, D., Arendt, K., Kim, D., 2020. All you need to know about model predictive control for buildings. Annu Rev Control 2020. 50, 190–

232. https://doi.org/10.1016/j.arcontrol.2020.09.001.
[5] Tahmasebinia, F., Lin, L., Wu, S., Kang, Y., Sepasgozar, S., 2023. Exploring the Benefits and Limitations of Digital Twin Technology in Building Energy. Appl. Sci. 13(15), 8814. https://doi.org/10.3390/app13158814
[6] Yang, B., Lv, Z., Wang, F., 2022. Digital Twins for Intelligent Green Buildings. Buildings 12(6), 856. https://doi.org/10.3390/buildings12060856
[7] de Wilde, P., 2023. Building performance simulation in the brave new world of artificial intelligence and digital twins: A systematic review. Energy Build. 292, 113171. https://doi.org/10.1016/j.enbuild.2023.113171.
[8] Pan, Y., Zhu, M., Lv, Y., Yang, Y., Liang, Y., Yin, R., Yang, Y., Jia, X., Wang, X., Zeng, F., Huang, S., Hou, D., Xu, L., Yin, R., Yuan, X., 2023. Building energy simulation and its application for building performance optimization: A review of methods, tools, and case studies. Advances in Appl. Energy, 10, 100135. https://doi.org/10.1016/j.adapen.2023.100135.
[9] Giannetti, N., Matsui, S., Mori, R., Jeong, J., Ariyadi, H., Miyaoka, Y., Togashi, E., Saito K., 2022a. Emulator-type load-based tests for dynamic performance characterization of air conditioners. Energy and Build. 273, 112411.
[10] Giannetti, N., Ariyadi, H., Miyaoka, Y., Jeong, J., Saito, K., 2022b. Development of an Emulator-Based Assessment Method for Representative Evaluation of the Dynamic Performance of Air Conditioners. International Refrigeration and Air Conditioning Conference. Paper 2448.
[11] Giannetti, N., Sholahudin, Mizuno, A., Miyaoka, Y., Sei, Y., Enoki, K., Saito, K., 2024. Feed-forward compensation for emulator-type testing facilities, Int. J. Refrig. 167, 257-268.
[12] Dondini, D., Giannetti, N., Mizuno, A., Miyaoka, Y., Saito, K., 2024. Reproducibility assessment of an emulator-type load-based testing methodology, Int. J. Refrig. 159, 39-49.
[13] NEEP. NEEP, 2023a. Final Report – Public Version, Residential Heat Pump Efficiency Rating Representativeness Project Phase 1.
[14] NEEP. NEEP, 2023b. Working title: Final Report, Residential Heat Pump Efficiency Rating Representativeness Project Phase 2.
[15] Harley, B., Dymond, C., Yuill, D., Hamer, G., McWilliams, J., Chen, Y., 2024. Field and Lab Testing of Residential Heat Pumps to Assess Representativeness of Fixed-speed and Load-based Test Methods, Proceedings of Purdue University, 2024 Herrick Refrigeration and Air Conditioning Conference.
[16] Miyaoka, Y., Mori, R., Giannetti, N., Jeong, J., Togashi, E., Saito, K., 2023. Emulator-type Load-based Testing Methodology for Dynamic Performance Characterization of Air Conditioners. Transactions of the Japan Society of Refrigerating and Air Conditioning

Engineers, e.22-17 _OA, February 2023. (in Japanese)
[17] Matsui, E., Kametani, S., 2020. Development of On-Site Performance Evaluation System for Multi-Air Conditioning Units in Buildings, Journal of Air Conditioning, Heating, and Sanitary Eng. 45, 282, 19-26.
[18] Sholahudin, Giannetti, N., Miyaoka, Y., Tanaka, K., Kowa, W., Saito, K., 2024. Implementation of scalable performance monitoring method for air conditioners, Appl. Therm. Eng. 245, 122820.
[19] Sholahudin, Giannetti, N., Miyaoka, Y., Saito, K., 2022. Intelligent performance prediction of air conditioning systems based on refrigerant temperatures, Thermal Science and Engineering Progress 27, 101150.
[20] Sholahudin, Giannetti, N., Saito, K., Yamaguchi, S., Saito, K., Tanaka, K., Ogami, H., 2020. A cost effective and non-intrusive method for performance prediction of air conditioners under fouling and leakage effect. Sustainable Energy Technologies and Assessments 42, 100856.
[21] Sholahudin, Giannetti, N., Yamaguchi, S., Saito, K., Miyaoka, Y., Tanaka, K., Ogami, H., Experimental implementation of artificial neural network for cost effective and non-intrusive performance estimation of air conditioning systems, Appl. Therm. Eng. 181, 115985.
[22] Sholahudin, Giannetti, N., Miyaoka, Y., Saito, K., Tanaka, K., Ogami, H., 2023. Experimental verification of artificial neural network scalability for performance monitoring of multi-split type air conditioners, Journal of Build. Eng. 76, 107427.
[23] Hosoi, A., Neto, A.H., Afshari, A., Wachau, A., Wang, B., Harley, B., Vering, C., Müller, D., Hogeling, J., Sager, J., Saito, K., Kurotori, K., Socal, L., Aye, L., Enteria, N., Giannetti, N., Kametani, S., Göbel, S., Sawachi, T., Kan, T., 2024. Evaluation and Demonstration of Actual Energy Efficiency of Heat Pump Systems in Buildings (Annex 88), State of the Art (Subtask A Report), Building Research Institute - National Research and Development Agency, Japan, Document Number: ISSN: 0453-4972.
[24] AQSIQ, 2018. Specification for Measurement of On-Site Performance Parameters of Air Conditioner (in Chinese).
[25] ANSI/ASHRAE, 2020. ANSI/ASHRAE Standard 221-2020. Test Method to Field-Measure and Score the Cooling and Heating Performance of an Installed Unitary HVAC System, 54 pages.
[26] Jactard, A., Li, Z., 2011. Investigation of field methods for evaluation of air-to-air heat pump performance, Master´s Thesis, Sustainable Energy Systems programme, Department of Energy and Environment, Division of Building Services Engineering, Chalmers University of Technology, 102 pages.
[27] Ichikawa, T., Yoshida, S., Nobe, T., Kametani, S., 2008. Running Performance of Split-

type Air Condition-ing Systems Installed in School and Office Buildings in Tokyo, International Refrigeration and Air Conditioning Conference. Paper 1003. http://docs.lib.purdue.edu/iracc/1003.
[28] Nobe, T., Haga, Y., Nakamura, H., Nobe, T., Haga, Y., Nakamura, H., Tanaka, K., Kiguchi, M., 2011. Probe insertion method for on-site evaluation of VRF system, Journal of Environmental Eng. (Transactions of AIJ) 76, 927-933. 10.3130/aije.76.927.
[29] Shimizu, S., Haga, Y., Yumoto, Y., Kametani, S., Nobe, T., 2006. Actual performance evaluation system of package air-conditioner by sampling system of heat rejection flux from outdoor unit, Part2: Accuracy verification of sampling system of heat rejection flux from outdoor unit in the calorie box, Tech. Pap. Annu. Meet. Soc. Heat. Air-Conditioning Sanit. Eng. Japan. (in Japanese).
[30] Shimizu, S., Haga, Y., Nobe, T., 2007. On-site Evaluation Method of Multi Split Air Conditioner System, Part 2: Investigation of Actual Efficiency by Sampling System. Journal of Asian Architecture and Building Eng. 6(2), 341-347.
[31] Haga, Y., Nobe, T., 2007. Accuracy Verification of Thermal Flux Sampler for Onsite Performance Evaluation of VRV System. In Proceedings of Clima 2007 WellBeing Indoors. Helsinki, Finland.
[32] Zhao, W., 2009. Study on Part Load Performance of Variable Refrigerant Flow System. Tsinghua Univer-sity, Master's Thesis, Beijing, China.
[33] Teodorese, V., Detroux, L., Lebrun, J., 2007. Testing of a Room Air Conditioner: High Class RAC Test Results - Medium Class RAC Test Results. University of Liege, Belgium.
[34] Tran, C.T., Rivière, P., Marchio, D., Arzano-Daurelle, C., 2012. Refrigerant-based measurement method of heat pump seasonal performances. Int. J. Refrig. 35(6), 1583–1594.
[35] Kim, W., Braun, J.E., 2016. Development and evaluation of virtual refrigerant mass flow sensors for fault detection and diagnostics. Int. J. Refrig. 63, 184–198.
[36] Fahlén, P., 1989. Capacity Measurement on Heat Pumps - A Simplified Measuring Method. Swedish Council for Building Research, Sweden.
[37] Zhang, G., Liu, W., Xiao, H., Shi, W., Wang, B., Li, X., 2019. New method for measuring field performance of variable refrigerant flow systems based on compressor set energy conservation. Appl. Therm. Eng. 154, 530–539.
[38] Yang, Z., Ding, L., Xiao, H., Zhang, G., Wang, B., Shi, W., 2020. All-condition measuring methods for field performance of room air conditioner. Appl. Therm. Eng. 180, 115887.
[39] Xiao, H., Shi, J., Yang, Z., Wang, B., Shi, W., Li, M., 2022. Precision improvement method for onsite performance measurement of variable refrigerant flow system. Building and Environment 208, 108626, https://doi.org/10.1016/j.buildenv.2021.108626.
[40] Takahashi, S., Kametani, S., Itou, M., Funatani, A., 2008. Study on Performance

Evaluation Method of a Split Air Conditioning System Based on Characteristic Curve of the Compressor Mass Flow Rate. In Proceedings of the International Refrigeration and Air Conditioning Conference. Purdue University, West Lafayette, IN, USA.
[41] Naruhiro, S., Shigeki, K., 2012. Study on the Development of the Performance Evaluation of VRF System Using the Volumetric Efficiency of the Compressor: Expansion of the Range of Application and Improvement of the Accuracy. In Proceedings of the Society of Heating, Air-Conditioning and Sanitary Engineers of Japan (SHASE).
[42] Lakshmi Narayana, T., Venkatesh, C., Ajmeera Kiran, Chinna Babu J., Adarsh Kumar, Surbhi Bhatia Khan, Ahlam Almusharraf, Mohammad Tabrez Quasim, 2024. Advances in real time smart monitoring of environmental parameters using IoT and sensors, Heliyon 10(7), e28195, https://doi.org/10.1016/j.heliyon.2024.e28195.
[43] Bandyopadhyay, M., Pal, S., Chattopadhyay, S., 2024. Development of an IoT based Environmental Pressure Monitoring System for prediction of Thunderstorm. *6th International Conference on Computational Intelligence and Networks (CINE)*, Bhubaneswar, India, 1-7, doi: 10.1109/CINE63708.2024.10881328.
[44] https://www.ams-ic.com.au/blog/back-to-basics-the-fundamental-measurements-of-pressure-in-industry/ Accessed on Sep. 25^{th} 2025.
[45] Arkhipov, A., Scarabosio, A., Haas, G., Mackel, F., Jürgen Koll, Meister, H., Eixenberger, H., Seyvet, F., Terron, S., Andrew, P., 2017. Status of the development of diagnostic pressure gauges for the operation in ITER. Fusion Engineering and Design 123, 1049-1053. https://doi.org/10.1016/j.fusengdes.2016.12.020.
[46] Tugova, E., Henry, M.P., Bushuev, O., Motorina, M., 2020. Development of a Wireless Pressure Transmitter with Diagnostics. 2020 Global Smart Industry Conference (GloSIC), Chelyabinsk, Russia pp. 204-209. doi: 10.1109/GloSIC50886.2020.9267829.
[47] Verbovšek, T., Šetina Batič, B., Šetina, J., Kokalj, T., 2017. A capillary manometer for pressure measurements in small cavities. Vacuum 138, 178-183, https://doi.org/10.1016/j.vacuum.2016.12.019.
[48] Du, P., Xue, J., Muñoz González, A., Luo, L., Woźny, P., Rodríguez-Mendoza, U.R., Lavín, V., Runowski, M., 2025. Highly pressure-responsive dual-mode optical manometer based on Mn2+-activated Ca2Gd8(SiO4)6O2 phosphors. Chem. Eng. J. 505, 159652, https://doi.org/10.1016/j.cej.2025.159652.
[49] Zanoni, B., Peri, C., Giovanelli, G., Pagliarini, E., 1998. Design and setting up of a water vapour pressure capacitance manometer for measurement of water activity. J. Food Eng. 38(4), 407-423, https://doi.org/10.1016/S0260-8774(98)00128-9
[50] K. O'Connell, 2001. TRANSDUCERS FOR ABSOLUTE MOTION. Editor(s): S. Braun, Encyclopedia of Vibration, Elsevier, 1381-1397, https://doi.org/10.1006/rwvb.2001.0103.

[51] Martin, J., Bacher, W., Hagena, O. F., Schomburg, W. K., 1998. Strain gauge pressure and volume-flow transducers made by thermoplastic molding and membrane transfer. *Proceedings MEMS 98. IEEE. Eleventh Annual International Workshop on Micro Electro Mechanical Systems. An Investigation of Micro Structures, Sensors, Actuators, Machines and Systems (Cat. No.98CH36176)*, Heidelberg, Germany, 1998, 361-366. doi: 10.1109/MEMSYS.1998.659783.

[52] https://www.sciencedirect.com/topics/engineering/strain-gage Accessed on Sep. 25th 2025.

[53] Fahle´n, P., 2004. Methods for Commissioning and Performance Checking of Heat Pumps and Refrigeration Equipment. Chalmers University of Technology, Gothenburg.

[54] Tran, C.T., Rivie`re, P., Marchio, D., Arzano-Daurelle, C., 2013. In situ measurement methods of air to air heat pump performance. Int. J. Refrig. 36, 1442-1455.

[55] Nwabueze, T.D., Zameroski, R., Gomez, M., Schmitz, T., 2025. Displacement measurement using various Hall effect sensor-magnet configurations. Manufacturing Letters 44, Supplement, 261-268. https://doi.org/10.1016/j.mfglet.2025.06.032.

[56] Bishop, A.I., Nieminen, T.A., Heckenberg, N.R., Rubinsztein-Dunlop, H., 2004. Optical Microrheology Using Rotating Laser-Trapped Particles. Phys. Rev. Lett. 92(19), 198104. doi:

[57] Tatzgern, F., Schirru, M., Schandl, M., Schneidhofer, C., Varga, M., 2025. Tribo-acoustic tachometer: A novel ultrasonic device for the simultaneous operando measurement of grease film thickness and cage rotational speed in rolling element bearings. Tribology International 212, 110930. https://doi.org/10.1016/j.triboint.2025.110930.

[58] Giannetti, N., Sholahudin, Miyaoka, Y., Saito, K., 2023. Novel performance monitoring technique for real-time estimation of end-user capacity supplied by vapour compression systems. JSRAE Annual Conference.

[59] Mao, G., Fujiwara, Ki, R.S., Serikawa, M., Sato, M., Mae, M., 2019. Benchmark test of simulation program applied for passive house design. Archit. Inst. Japan Technical Rep. Collect., 25(61), 1185-1190. (In Japanese)

[60] https://www.mlit.go.jp/common/000995432.pdf (last accessed on 26/07/2022). (In Japanese).

[61] Sakai, Y., Unishi, H., Yahata, T., 2004. Non-destructive Method of Stress Evaluation in Linepipes Using Magnetic Anisotropy Sensor, JFE TECHNICAL REPORT No. 3.

[62] Zhu, X.K., 2023. Exact solution of burst pressure for thick-walled pipes using the flow theory of plasticity. Int. J. Mech. Sc. 259, 108582. https://doi.org/10.1016/j.ijmecsci.2023.108582.

[63] https://uk.rs-online.com/web/p/strain-gauges/0632168 Accessed on Sep. 25th 2025.

[64] Lemmon, E.W., Bell, I.H., Huber, M.L., McLinden, M.O., 2018. NIST Standard

Reference Database 23: Reference Fluid Thermodynamic and Transport Properties-REFPROP, Version 10.0, National Institute of Standards and Technology, Standard Reference Data Program, Gaithersburg.
[65] Surhone, L.M., Timpledon, M.T., Marseken, S.F., 2010. Nyquist-Shannon Sampling Theorem. Betascript Publishing.